DIGITAL ACCESS TO SCHOLARSHIP AT HARVARD
DASH.HARVARD.EDU

HARVARD LIBRARY
Office for Scholarly Communication

Dextran-Coated Iron Oxide Nanoparticles: a Versatile Platform for Targeted Molecular Imaging, Molecular Diagnostics and Therapy

Citation

Tassa, Carlos, Stanley Y. Shaw, and Ralph Weissleder. 2011. "Dextran-Coated Iron Oxide Nanoparticles: A Versatile Platform for Targeted Molecular Imaging, Molecular Diagnostics, and Therapy." Accounts of Chemical Research 44 (10): 842–52. https://doi.org/10.1021/ar200084x.

Permanent link

http://nrs.harvard.edu/urn-3:HUL.InstRepos:41384288

Terms of Use

This article was downloaded from Harvard University's DASH repository, and is made available under the terms and conditions applicable to Other Posted Material, as set forth at http://nrs.harvard.edu/urn-3:HUL.InstRepos:dash.current.terms-of-use#LAA

Share Your Story

The Harvard community has made this article openly available.
Please share how this access benefits you. Submit a story .

Accessibility

NIH Public Access
Author Manuscript
Acc Chem Res. Author manuscript; available in PMC 2011 October 19.

Published in final edited form as:
Acc Chem Res. 2011 October 18; 44(10): 842–852. doi:10.1021/ar200084x.

Dextran-Coated Iron Oxide Nanoparticles: a Versatile Platform for Targeted Molecular Imaging, Molecular Diagnostics and Therapy

Carlos Tassa, **Stanley Y. Shaw**, and **Ralph Weissleder***
Center for Systems Biology Massachusetts General Hospital and Harvard Medical School, Boston, Massachusetts

1. INTRODUCTION

Advances in our understanding of the genetic basis of disease susceptibility, coupled with prominent successes for molecular targeted therapies, have resulted in an emerging strategy of personalized medicine. This approach envisions risk stratification and therapeutic selection based on an individual's genetic makeup and physiologic state (the latter assessed through cellular or molecular phenotypes). Molecularly targeted nanoparticles can play a key role in this vision through non-invasive assessments of molecular processes and specific cell populations in vivo, sensitive molecular diagnostics ex vivo, and targeted delivery of therapeutics.[1-3] Derivatized dextran coated magnetic nanoparticles[4, 5] are a powerful platform for these applications, as they support diagnostic imaging by magnetic resonance (MRI), optical and PET modalities, and constitute a versatile platform for conjugation to targeting ligands. Pharmacokinetic and toxicity studies have revealed these nanomaterials to be sufficiently non-toxic and biodegradable[6, 7] with extended vascular retention times. Certain nanoparticles of this class are now FDA-approved.

Experimental dextran-coated superparamagnetic iron oxide nanoparticles are a well-established platform for the synthesis of multifunctional imaging agents. These include monocrystalline iron oxide nanoparticles (or MION)[8, 9] and the related nanoparticles where the dextran is covalently cross-linked (cross-linked iron oxide nanoparticles, or CLIO) to form amine groups that are ready substrates for conjugation to targeting ligands. Several nanoparticles with iron cores and carbohydrate coatings have been approved for human use. In 1996, the US Food and Drug Administration (FDA) approved Feridex I.V.® (ferumoxides) as the first nanoparticle-based iron oxide imaging agent for the detection of liver lesions. A smaller monodisperse version, Combidex® (ferumoxtran-10) has been used to image occult prostate cancer lymph-node metastases in humans. Finally, Feraheme® (ferumoxytol) has been approved to treat iron deficiency anemia in adult patients with chronic kidney disease. Ferumoxytol is also under clinical investigation for the detection of central nervous system (CNS) inflammation, brain neoplasms and cerebral metastases from lung or breast cancer.

This account will describe our recent efforts in the development of an integrated system of nanoparticles, conjugation chemistries, screening methods, and detection technologies, with wide applications in biologic discovery, molecular imaging, diagnostic analyte detection, and therapeutic decision-making and monitoring.

*To whom correspondence should be addressed. rweissleder@mgh.harvard.edu .

NIH-PA Author Manuscript
NIH-PA Author Manuscript
NIH-PA Author Manuscript

NIH-PA Author Manuscript

NIH-PA Author Manuscript

NIH-PA Author Manuscript

2. CLIO PLATFORM

Superparamagnetic iron oxide nanoparticles are typically produced by one of two different mechanisms: i) high temperature hydrophobic crystal growth and subsequent coating with biocompatible polymers [10-13] or ii) precipitation from an alkaline solution containing a mixture of iron salts (Fe^{2+}, Fe^{3+}) and a coating polymer such as dextran.[4] The former generally results in highly monodisperse, high relaxivity materials primarily used for in vitro applications,[14] and the latter results in much more biocompatible materials for in vivo use.[6, 15, 16]

MION are produced by the second method and contain a 3-5 nm monocrystalline core surrounded by a layer of dextran of variable thickness. The overall mean hydrated diameter typically falls within the 20-45 nm range. Since the iron core and dextran shell are held together via noncovalent binding interactions, core-shell dissociation may occur under certain biological conditions. To prevent dextran dissociation and introduce a convenient functional group for multivalent conjugation, MION can be treated with epichlorohydrin to crosslink the dextran coating (resulting in crosslinked iron oxide nanoparticles, or CLIO) followed by treatment with ammonia to introduce primary amines (CLIO-NH_2).[8, 9] The primary amines distributed throughout the nanostructure allow increased loading capacity for the attachment of multiple targeting ligands, imaging agents and therapeutics into one entity. An alternative to chemical cross-linking is the use of carboxylated dextrans as the primary coating.[17, 18]

3. CHEMISTRY

Efficient conjugation chemistry methods have extended the versatility of the CLIO platform for multiple applications. Straightforward protocols exist to conjugate ligands bearing a variety of functional groups to the primary amines on CLIO's dextran coating, including anhydrides, amines, hydroxyls, carboxylic acids, thiols, and epoxides. (Figure 1) Recently, a bioorthogonal [4 + 2] cycloaddition reaction between 1,2,4,5-tetrazene (Tz) and *trans*-cyclooctene (TCO) was described that can label cancer cells, peptides and small molecules.[19-21] (Figure 2) The reaction does not require catalyst, and proceeds rapidly at room temperature with high yields in a variety of solvents including serum. A novel labeling strategy termed BOND for 'bioorthogonal nanoparticle detection' uses this mechanism to conjugate nanoparticles to targeting ligands such as antibodies (Figure 2).[22, 23] Antibodies are modified with TCO moieties at lysine residues. TCO-modified antibodies can then be reacted with Tz-derivatized nanoparticles, resulting in multivalent nanoparticles bearing multiple copies of targeting ligands (e.g. antibodies, peptides or small molecules). To maximize the amplification conferred by multivalent attachment, it may be advantageous to use reactants and ligands that impose minimal steric hindrance (small 'footprints') and allow a maximal number of covalent attachment sites on the nanoparticle. BOND type chemistry enables efficient targeting and signal amplification for a wide variety of diagnostic and detection applications.[24-28]

4. SMALL-MOLECULE MODIFIED NANOPARTICLE LIBRARIES

While most CLIO-based applications to date have utilized peptides or antibodies for targeting, surface modification through multivalent attachment of small molecules holds great potential for selective targeting of cell types. The flexible CLIO platform enables a screening approach to be extended to libraries of small molecule-modified nanoparticles, i.e. phenotypic screens to identify targeted nanoparticles with specificity for a cell-type of interest (and without *a priori* knowledge of the protein target). Phenotype-driven screens of nanoparticle libraries are a powerful complement to traditional target-based nanoparticle design, and may enable targeting of a broader range of cell types of interest.

NIH-PA Author Manuscript

NIH-PA Author Manuscript

NIH-PA Author Manuscript

As an example, amino CLIO (bearing ~ 62 free amines) was sparsely labeled with the near IR fluorochrome Cy5.5. Remaining free amines were conjugated to 146 different small molecules (MW < 500 Da) selected based on water solubility and chemical diversity.[29] While the starting CLIO nanoparticle is taken up exclusively by macrophages, screening in different cell lines and subsequent studies showed that glycine-modified CLIO specifically labeled functional macrophage subsets, such as a subset of tumor-associated macrophages with proangiogenic and immunosuppressive properties.[30]

While the above study narrowed nanoparticle targeting from all macrophages to a functional macrophage subset, a longterm goal is to enable targeting of non-macrophage cell types. A subsequent study demonstrated the viability of this approach, by screening for small molecule-modified nanoparticles with enhanced binding to vascular endothelial cells. The robustness of the screen was increased by several design elements a) using primary isolates of human endothelial cells (rather than cell lines), b) screening multiple independent isolates of endothelial cells from multiple vascular beds (to avoid skewing screening results by a single idiosyncratic cell isolate, and enhance the generality of screening "hits"), and c) by adopting rigorous analytic methods for the multidimensional data set.[31] Nanoparticles were screened for enhanced binding to 11 isolates of vascular endothelial cells (the target class), while minimizing binding to 2 isolates of macrophages (background class). A t-statistic was calculated for each nanoparticle, which reflects the extent that the nanoparticle shows a difference in binding to endothelial cells, compared to its binding to macrophages. The statistical significance for each nanoparticle was evaluated using permutation-based p-values (Figure 3). From the 'hits' from the initial screen ($p \leq 3\times10^{-3}$), selected nanoparticles were validated by demonstrating enhanced localization to endothelium in two physiologic contexts: human carotid endarterectomy samples (from operating room specimens), and intravital imaging of murine blood vessels *in vivo*. Thus, phenotypic cell-based screening of nanoparticle libraries across target vs. background cell types, combined with appropriate analytic methods, led to the discovery of imaging probes with novel properties.

These unbiased screening approaches can be extended to identify probes for a wide variety of cell types of interest. In the context of personalized medicine, one could envision screens for imaging probes that distinguish cells defined by a difference in phenotype (e.g. low vs. high metastatic potential) or genotype (e.g. expressing a risk allele vs. a protective allele at a disease gene).

5. LIGAND EFFECTS ON NANOPARTICLE BINDING

Targeted nanoparticles are widely thought to benefit from multivalent interactions, where multiple ligands on the nanoparticle simultaneously bind to multiple receptors on another entity (e.g. a cell surface, or a multimeric protein).[32] However, given the complexities inherent in the interactions of nanoparticle surfaces with their targets, and the structural diversity of nanoparticle scaffolds and targeting ligands, our understanding of how the multivalent display of targeting ligands affects nanoparticle binding remains incomplete. Furthermore, the effects of multivalency on nanoparticle binding are often not quantitated, or are measured indirectly through cell-based assays.

To address these issues, we used surface plasmon resonance (SPR) to directly quantitate the affinity and kinetics of nanoparticle-target interactions in real time.[33] We studied a deliberately constrained system where CLIO was conjugated to a series of structurally related synthetic analogs that all bound the same target, FK506-binding protein 12 (FKBP12). The K_D's for the free FKBP12 ligands span a 4500-fold range (24 nM to 110 uM). These FKBP12 ligands were conjugated to CLIO using sulfhydryl exchange chemistry, which allowed quantitative determination of ligand loading and thus nanoparticle

NIH-PA Author Manuscript

NIH-PA Author Manuscript

NIH-PA Author Manuscript

multivalency (ranging from ~3-18 ligands/CLIO). At high receptor (FKBP12) densities typically used for SPR experiments, multivalent interactions resulted in negligible dissociation rates (k_d). However, at lower, physiologically relevant receptor densities (comparable to measured receptor densities on cancer cells), several notable findings resulted (Figure 4). As expected, dissociation rates k_d between the multivalent nanoparticle and FKBP12 were significantly reduced relative to the free small molecule ligands. Less expected was the considerable variation in association rates, as k_a for the nanoparticle-FKBP12 interaction increased, decreased or remained largely unchanged relative to the free small molecules. Quantitative curve-fitting of SPR responses confirmed that increasing contributions from multivalent (as opposed to monovalent) interactions correlated with increased binding affinity and avidity. Parallel analyses showed that structural components such as linker length and conjugation chemistry could also influence binding kinetics of multivalent nanoparticles in unexpected ways.

The kinetic insights uncovered by our SPR measurements at physiologically relevant receptor densities could have important functional implications. First, they suggest that nanoparticle design may not always be straightforwardly modular, as the details of how a nanoparticle is conjugated to a targeting ligand influenced nanoparticle behavior. Second, they argue that direct measurement of nanoparticle binding affinities and kinetics can inform nanoparticle design. For instance, nanoparticle affinity, and association and dissociation rates can all affect how deeply an intravascular circulating agent penetrates into tissue before its target sites become effectively saturated;[34] the relative contribution of these variables depends on several *in vivo* factors, including capillary permeability, particle size and target density. In light of this, two targeted nanoparticles that have comparable equilibrium affinities for their target may possess very distinct kinetic properties with functional consequences. More broadly, SPR can guide the design, synthesis and structure-activity studies of functionalized nanoparticles for a variety of ligand, scaffold and target combinations.

6. BIOMEDICAL APPLICATIONS

Progress in the syntheses of nano-scale materials is envisioned to play a critical role in the development of novel diagnostics and therapeutics. Derivatized magnetic nanoparticles (with carbohydrate coatings such as dextran) possess many properties that make them well-suited for these applications. The superparamagnetic iron oxide core enables *in vivo* imaging by magnetic resonance. Clustering of nanoparticles can be used as the basis for highly sensitive *ex vivo* analyte detection in point-of-care devices. The nanoparticle surfaces are readily modified with targeting ligands, and can benefit from enhanced avidity conferred by multivalency. Antibody, peptide and/or small molecule derivatized magnetic nanoparticles have all been developed successfully. The particles are biocompatible, with favorable circulating half-lives. For all of these reasons, these nanoparticles are widely utilized in translational cell- and animal-based experiments, and certain nanoparticles of this class are now FDA approved for human use. The sections below briefly summarize some recent highlights; further details may be found in several reviews.[2, 35, 36]

6.1 DIAGNOSTIC MAGNETIC RESONANCE (DMR)

The ability to detect specific analytes in a sensitive and efficient manner is critical for point of care tests for diagnosis, prognosis and monitoring of disease activity and therapeutic efficacy. Ideal biosensors should provide rapid, high sensitivity detection and quantitation of a range of different analytes, with low sample volume requirements and cost. An innovative approach for detecting analytes takes advantage of CLIO-like nanoparticles and magnetic self-amplifying proximity effects[37] or magnetic tagging.[14, 38, 39] In either mode, the presence of the target analyte induces target-mediated nanoparticle clustering, resulting in

NIH-PA Author Manuscript

NIH-PA Author Manuscript

NIH-PA Author Manuscript

decreased T_2 relaxation times or increased relaxation rates R_2 ($R_2 = 1/T_2$) of neighboring water molecules relative to monodisperse nanoparticles (forward magnetic relaxation switching, or MRS). Several different types of molecular interactions have been detected using MRS and bench-top relaxometers, including DNA-DNA, protein-protein, protein-small molecule, enzymatic activity via reverse assay, telomerase activity and bacterial detection.[37, 4041-45] Significantly, these can be detected in turbid media and whole cell lysates; the lack of purification is a critical advantage for processing of clinical samples such as blood. In a recent study addressing the effects of multivalency on the binding and detection of cells using magnetic relaxation nanosensors, high valency nanoparticles outperformed the low valency counterpart, achieving rapid single cell detection. [46] Additionally, multivalent nanosensors have been used as molecular mimics for toxin detection. [47]

Miniaturization of the magnetic resonance components has resulted in a field-ready diagnostic magnetic resonance (DMR) device.[38] The first prototype, DMR-1, incorporates a microcoil array, microfluidic network, electronics and permanent magnet, all in a portable self-contained assembly. Onboard custom electronics provide both longitudinal (T_1) and traverse (T_2) relaxation time measurements. Side-by-side performance comparisons between a benchtop relaxometer, and DMR-1 showed less than 2% difference in measured *R*1 and *R*2 values. (relaxation per iron concentration in water). Moreover, DMR-1 mass detection sensitivity improved 80-fold over the relaxometer, due mainly to device miniaturization which enables stronger radio frequency field generation with increased filling factors in small sample volumes.

A second generation device, DMR-2, improved detection sensitivity.[14] First, the probe design was changed to a solenoid microcoil probe embedded in a microfluidic structure to decrease sample volume and improve signal to noise ratio (SNR). The second improvement took advantage of novel water-soluble magnetic nanoparticles (MNP) with significantly greater r_2 relaxivities (high r_2 will induce large R_2 changes) which were synthesized by doping iron oxide nanoparticles with manganese (Mn-MNP) and using seed-growth techniques to increase overall metallic core size. In fine needle aspirates (FNAs) from xenograft mouse tumors, DMR-2 combined with anti-Her2/neu-Mn-MNP nanoparticles resulted in a linear relationship between traverse relaxation rate R_2 and Her2/neu$^+$ cell counts, with a detection limit of ~2 cells per 1 uL sample (far below that of standard-of-care methods such as histology).

Finally, a third generation device (DMR-3) is an integrated, clinical micro-NMR (μNMR) device capable of rapid and quantitative profiling of multiple protein markers.[48] (Figure 5) DMR-3 includes the capability to perform multiplexed analyte measurement, microfluidic specimen delivery, increased temperature stability, and can be controlled via a smart-phone application. Cells from FNAs for suspected human abdominal malignancies were first labeled by a TCO-modified antibody against the cancer marker, followed by labeling with Tz-modified magnetic nanoparticles. This system was first used to profile 9 different cancer markers in 50 patients undergoing abdominal FNA. (Figure 6) NMR signals for the cancer markers showed very high correlation with gold-standard methods of clinical measurement, such as flow cytometry or immunohistochemistry. Using standard-of-care clinical assessments classifying each tumor as benign or malignant as the gold standard, a weighted 4-marker profile (composed of MUC-1, EGFR, HER2, and EpCAM) showed 96% accuracy. In an independent cohort of 20 patients, this four-marker panel showed 100% accuracy in classifying samples as benign or malignant. Of note, marker measurements by NMR were available in less than one hour, while standard processing required 3-4 days on average and often longer. Thus, sensitive detection of cells from human FNAs using DMR-3 and magnetic nanoparticles can enable patient phenotyping based on profiles of expressed cancer

NIH-PA Author Manuscript

NIH-PA Author Manuscript

NIH-PA Author Manuscript

markers. DMR-3 enables a binary diagnostic distinction (benign vs. malignant), but the underlying approach is adaptable to multiplex phenotyping of patient tumors for tumor classification, risk stratification, and monitoring response to therapy.

6.2 MAGNETIC RESONANCE IMAGING (MRI)

The ability to image CLIO and related nanoparticles by magnetic resonance has led to several probes that image cellular and subcellular events with high spatial resolution,[6, 17, 49-65] and can be used for early diagnosis, risk stratification, and monitoring of disease activity or therapeutic efficacy. For example, a magnetofluorescent nanoparticle targeted to vascular adhesion molecule-1 (VCAM-1) was designed to image atherosclerosis in vivo.[60] Upregulation of vascular adhesion molecule-1 (VCAM-1) on activated endothelial cells, macrophages and smooth muscle cells is an early marker of atherosclerosis. A VCAM-1 targeting peptide was selected utilizing iterative phage display, and conjugated to CLIO. Intravenous administration of this targeted particle results in enhanced MR signal in aortic roots of apoE$^{-/-}$ mice, which correlated with VCAM-1 expression. This probe was also useful for in vivo monitoring of therapeutic efficacy, as evidenced by improved signal after statin treatment.

In another example, a similar magnetofluorescent nanoparticle was designed to visualize apoptosis. Phosphatidylserine becomes externalized on cell membranes early in the apoptotic process, and annexin V binds phosphatidylserine. CLIO conjugated to annexin V has been shown to be a sensitive indicator of cardiomyocyte apoptosis in vivo.[62-64]

6.3 POSITRON EMISSION TOMOGRAPHY (PET) IMAGING

Positron emission tomography (PET) imaging identifies high-energy photons from trace quantities of decaying radioactive isotopes with significantly higher sensitivity than MRI. Labeling of nanoparticles with PET isotopes such as ^{18}F has been successfully used to decrease both the detection threshold and the clinical dose required. Using copper-catalyzed azide-alkyne cycloaddition (“click” chemistry), a fluorescently-derivatized CLIO was conjugated with ^{18}F to create a trimodal nanoparticle that can be detected by PET, fluorescence molecular tomography (FMT) and MRI. (Figure 7) The detection threshold for ^{18}F-CLIO by PET was 200 times more sensitive than MRI [16] and 50 times more sensitive than FMT. In agar-based phantoms, CLIO-based particles bearing ^{18}F and the fluorescent dye VT680 show excellent correlation between PET and FMT signals ($r^2 > 0.99$).

CLIO-based PET/FMT/MRI imaging agents offer the prospect of sensitive, multichannel assessments of different biological signals in vivo. In a CT26 colon carcinoma mouse xenograft model, ^{64}Cu-CLIO-VT680 showed good correlation of PET and FMT signals ($r^2 = 0.82$) within tumor volumes, corresponding to CLIO targeting of tumor-associated macrophages. For multichannel imaging in vivo, the ^{64}Cu-CLIO-VT680 particle was co-injected with a fluorescent probe for cathepsin enzymatic activity, and a fluorescent probe for αvβ3 integrins. Spectrally resolved signals were observed within tumors in vivo, with different agents localizing to distinct subregions of the tumor according to their biological targets.[66] (Figure 7)

PET-CT imaging of ^{18}F-CLIO resulted in significantly higher PET signal in murine aortic aneurysms compared to normal aorta, due to ^{18}F-CLIO targeting of monocytes and macrophages within the aneurysm. Cellular probe distribution was validated by radionuclide, fluorescence, histologic and flow cytometric measurements. Currently, decisions on surgical resection of aneurysms are based on population-derived risk factors such as aneurysm diameter. Nanoparticle-PET agent conjugates may allow individualized

NIH-PA Author Manuscript

NIH-PA Author Manuscript

NIH-PA Author Manuscript

therapeutic decisions, based on molecular disease markers such as cellular inflammatory activity in the aneurysm.[67]

6.4 THERANOSTIC PARTICLES: PHOTODYNAMIC THERAPY (PDT)

Various formulations of iron oxide-based nanoparticles have been developed for theranostic applications, in which the nanoparticle carries imaging, targeting and therapeutic capabilities. For instance, iron oxide nanoparticles were synthesized with a polyacrylic acid (PAA) polymer coating that encapsulated a near infrared dye and the chemotherapeutic drug Taxol. Functionalization of this nanoparticle with folate allowed uptake into A549 lung cancer cells, Taxol release and cell death.[68] Nanoparticle-borne payloads have included genes, proteins, drugs, or combinations thereof, which have recently been reviewed.[69]

PDT is a promising treatment modality for several types of diseases including artherosclerosis and cancer.[70] PDT uses a photosensitizer-based drug, oxygen and light of a specific wavelength to produce singlet oxygen, a highly reactive species that causes proximity-based photonecrotic effects. By directing light of a specific wavelength to a precise region, PDT can cause localized tumor killing without damaging nearby healthy tissue. A drawback to systemically-delivered photosensitizers, however, is skin accumulation leading to photosensitivity.

CLIO has proven to be an appealing theranostic platform to deliver photosensitizing agents in a targeted fashion, decreasing photosensitivity complications. Hydroporphyrins of the chlorin class sensitize formation of singlet oxygen and have been used extensively in PDT applications.[71] In a first generation multimodal theranostic nanoparticle (TNP), CLIO was conjugated to the potent photosensitizer tetraphenyl-2,3-dihydroxychlorin (TPC) (with singlet oxygen quantum yield = 0.65 (645 nm excitation)), and also to Alexa Fluor 750 for fluorescent localization.[72] The resulting TNP had a characteristic uv-vis absorption spectrum featuring all three optically active components (CLIO abs <400 nm, TPC abs = 650 and Alexa Fluor 750 abs = 750). The 100 nm differences in absorption between TPC and Alexa Fluor 750 minimized energy transfer and singlet oxygen generation during optical imaging. In a macrophage cell line, irradiation with 650 nm light resulted in dose-dependent phototoxicity, whereas irradiation at 750 nm for optical imaging did not cause any observable cell death.

A second-generation TNP conjugated the hydrophilic *meso*-tetra(hydroxyphenyl)-2,3-dihydroxychlorin (THPC) to CLIO, which allowed for 3-fold greater nanoparticle loading.[73] The resulting CLIO-THPC had improved aqueous stability and almost 60 times greater phototoxicity than conventional chlorin e_6. (Figure 8) In an apolipoprotein E-deficient mouse model of atherosclerosis, CLIO-THPC localized to carotid artery atheroma (specifically areas rich in macrophages and foam cells). Surgically exposed carotid arteries were irradiated with 650 nm light, incisions were closed and mice were allowed to recuperate. Follow-up tissue staining showed extensive macrophage cell death and apoptosis in atheroma. (Figure 8) CLIO-THPC caused significantly less skin phototoxicity in mice compared to chlorin e_6, validating the benefit of nanoparticle-targeted PDT.

7. CONCLUSIONS

The platform of dextran-coated iron oxide nanoparticles has proven to be an important part of the armamentarium for multiple phases of personalized medicine (i.e. therapy chosen to match individual genotype or phenotype). The large cargo capacity and suitability for a variety of conjugation methods has enabled CLIO's use for molecular imaging, sensitive and rapid ex vivo detection of analytes, and the targeted delivery of therapy. Ongoing and future efforts will extend the lessons learned with CLIO to clinical grade iron oxide nanoparticles,

NIH-PA Author Manuscript

NIH-PA Author Manuscript

NIH-PA Author Manuscript

such as those based on ferumoxides, ferumoxtran-10 or ferumoxytol. Also, the reproducible synthesis of derivatized nanoparticles designed for human applications needs to be standardized. Targeting ligands will be developed against a wider range of cellular proteins, enabling applications in a wider range of diseases. Finally, studies of nanoparticles in cohorts of human subjects are needed to rigorously assess the potential of these nanoparticles to function as clinically relevant biomarkers. Ultimately, these types of nanoparticles show great potential to participate in many steps in the cycle of personalized care, including individualized risk stratification, early diagnosis, and assessment of disease activity. Such personalized phenotyping can subclassify patients to identify new endophenotypes, and match patients with the most appropriate therapy.

Acknowledgments

The authors gratefully acknowledge the contributions from all researchers whose work has been described in this account. This work was funded by contract number HHSN268201000044C (NIH/NHLBI) to S.Y.S. and R.W.

BIOGRAPHICAL INFORMATION

Carlos Tassa is a Research Scientist in the Center for Systems Biology at Massachusetts General Hospital (MGH). He received his B.S and M.S. in Chemistry from the University of Massachusetts Boston, working under the guidance of John C. Warner. Following his Ph.D. studies in synthetic organic chemistry at Dartmouth College with Peter A. Jacobi, he pursued post doctoral training in the Chemical Biology Program at the Broad Institute of Harvard and MIT under Stanley Shaw and Stuart Schreiber.

Stanley Y Shaw is a Principal Investigator and Co-Director of Chemical Biology in the MGH Center for Systems Biology, and an Assistant Professor at Harvard Medical School . He received his A.B. in Chemistry & Physics, M.D. and Ph.D. at Harvard; his Ph.D. in Biophysics studied DNA topology under the supervision of James Wang. He worked with Stuart Schreiber as a Howard Hughes Medical Institute physician post-doctoral fellow. His laboratory seeks to develop a variety of approaches to phenotype human patients and correlate these phenotypes with their genetic susceptibility to disease. These goals are pursued using molecular imaging, phenotyping of patient-derived cells, chemical biology, and extracting phenotypes from electronic health records (EHR) using natural language processing.

Ralph Weissleder is a Professor of Systems Biology and of Radiology at Harvard Medical School, and Director of the Center for Systems Biology at Massachusetts General Hospital (MGH). Dr. Weissleder is a graduate of the University of Heidelberg. He has received many awards including the J. Taylor International Prize in Medicine, the Millenium Pharmaceuticals Innovator Award, the AUR Memorial Award, the ARRS President's Award, The Society for Molecular Imaging Lifetime Achievement Award, and the Academy of Molecular Imaging 2006 Distinguished Basic Scientist Award. In 2009 he was elected to the Institute of Medicine in the United States National Academies. His lab has been a driving force in studying human biology using molecular imaging and nanotechnology, with a particular focus on cancer and inflammatory diseases. He has developed systematic ways to explore disease biology using in vivo imaging and has been instrumental in translating several discoveries into new drugs.

REFERENCES

1. Jaffer FA, Weissleder R. Molecular imaging in the clinical arena. JAMA. 2005; 293(7):855–862. [PubMed: 15713776]

NIH-PA Author Manuscript

NIH-PA Author Manuscript

NIH-PA Author Manuscript

2. McCarthy JR, Weissleder R. Multifunctional magnetic nanoparticles for targeted imaging and therapy. Adv Drug Deliv Rev. 2008; 60(11):1241–1251. [PubMed: 18508157]
3. Weissleder R. Molecular imaging in cancer. Science. 2006; 312(5777):1168–1171. [PubMed: 16728630]
4. Shen T, Weissleder R, Papisov M, Bogdanov AJ, Brady TJ. Monocrystalline iron oxide nanocompounds (MION): physicochemical properties. Magn Reson Med. 1993; 29(5):599–604. [PubMed: 8505895]
5. Weissleder R, Bogdanov A, Neuwelt EA, Papisov M. Long-circulating iron oxides for MR imaging. Adv Drug Del Rev. 1995; 16:321–334.
6. Harisinghani MG, Barentsz J, Hahn PF, Deserno WM, Tabatabaei S, van de Kaa CH, de la Rosette J, Weissleder R. Noninvasive detection of clinically occult lymph-node metastases in prostate cancer. N Engl J Med. 2003; 348(25):2491–2499. [PubMed: 12815134]
7. Weissleder R, Stark DD, Engelstad BL, Bacon BR, Compton CC, White DL, Jacobs P, Lewis J. Superparamagnetic iron oxide: pharmacokinetics and toxicity. AJR Am J Roentgenol. 1989; 152(1): 167–173. [PubMed: 2783272]
8. Josephson L, Tung CH, Moore A, Weissleder R. High-efficiency intracellular magnetic labeling with novel superparamagnetic-Tat peptide conjugates. Bioconjug Chem. 1999; 10(2):186–191. [PubMed: 10077466]
9. Wunderbaldinger P, Josephson L, Weissleder R. Crosslinked iron oxides (CLIO): a new platform for the development of targeted MR contrast agents. Acad Radiol. 2002; 9(Suppl 2):S304–6. [PubMed: 12188255]
10. Park J, An K, Hwang Y, Park JG, Noh HJ, Kim JY, Park JH, Hwang NM, Hyeon T. Ultra-large-scale syntheses of monodisperse nanocrystals. Nat Mater. 2004; 3(12):891–895. [PubMed: 15568032]
11. Sun S, Zeng H, Robinson DB, Raoux S, Rice PM, Wang SX, Li G. Monodisperse MFe2O4 (M = Fe, Co, Mn) nanoparticles. J. Am. Chem. Soc. 2004; 126(1):273–279. [PubMed: 14709092]
12. Hyeon T, Lee SS, Park J, Chung Y, Na HB. Synthesis of highly crystalline and monodisperse maghemite nanocrystallites without a size-selection process. J. Am. Chem. Soc. 2001; 123(51): 12798–12801. [PubMed: 11749537]
13. Park J, Joo J, Kwon SG, Jang Y, Hyeon T. Synthesis of monodisperse spherical nanocrystals. Angew Chem Int Ed Engl. 2007; 46(25):4630–4660. [PubMed: 17525914]
14. Lee H, Yoon TJ, Figueiredo JL, Swirski FK, Weissleder R. Rapid detection and profiling of cancer cells in fine-needle aspirates. Proc. Natl. Acad. Sci. U. S. A. 2009; 106(30):12459–12464. [PubMed: 19620715]
15. Weissleder R, Moore A, Mahmood U, Bhorade R, Benveniste H, Chiocca EA, Basilion JP. In vivo magnetic resonance imaging of transgene expression. Nat Med. 2000; 6(3):351–355. [PubMed: 10700241]
16. Devaraj NK, Keliher EJ, Thurber GM, Nahrendorf M, Weissleder R. 18F labeled nanoparticles for in vivo PET-CT imaging. Bioconjug Chem. 2009; 20(2):397–401. [PubMed: 19138113]
17. Harisinghani M, Ross RW, Guimaraes AR, Weissleder R. Utility of a new bolus-injectable nanoparticle for clinical cancer staging. Neoplasia. 2007; 9(12):1160–1165. [PubMed: 18084623]
18. Liong M, Shao H, Haun JB, Lee H, Weissleder R. Carboxymethylated polyvinyl alcohol stabilizes doped ferrofluids for biological applications. Adv Mater. 2010; 22(45):5168–5172. [PubMed: 20859943]
19. Blackman ML, Royzen M, Fox JM. Tetrazine ligation: fast bioconjugation based on inverse-electron-demand Diels-Alder reactivity. J. Am. Chem. Soc. 2008; 130(41):13518–13519. [PubMed: 18798613]
20. Devaraj NK, Upadhyay R, Haun JB, Hilderbrand SA, Weissleder R. Fast and sensitive pretargeted labeling of cancer cells through a tetrazine/trans-cyclooctene cycloaddition. Angew Chem Int Ed Engl. 2009; 48(38):7013–7016. [PubMed: 19697389]
21. Devaraj NK, Weissleder R, Hilderbrand SA. Tetrazine-based cycloadditions: application to pretargeted live cell imaging. Bioconjug Chem. 2008; 19(12):2297–2299. [PubMed: 19053305]

NIH-PA Author Manuscript

NIH-PA Author Manuscript

NIH-PA Author Manuscript

22. Haun JB, Devaraj NK, Hilderbrand SA, Lee H, Weissleder R. Bioorthogonal chemistry amplifies nanoparticle binding and enhances the sensitivity of cell detection. Nat Nanotechnol. 2010; 5(9): 660–665. [PubMed: 20676091]
23. Haun JB, Devaraj NK, Marinelli BS, Lee H, Weissleder R. Probing intracellular biomarkers and mediators of cell activation using nanosensors and bioorthogonal chemistry. ACS Nano. 2011; 5(4):3204–3213. [PubMed: 21351804]
24. Han HS, Devaraj NK, Lee J, Hilderbrand SA, Weissleder R, Bawendi MG. Development of a bioorthogonal and highly efficient conjugation method for quantum dots using tetrazine-norbornene cycloaddition. J. Am. Chem. Soc. 2010; 132(23):7838–7839. [PubMed: 20481508]
25. Keliher EJ, Reiner T, Turetsky A, Hilderbrand SA, Weissleder R. High-Yielding, Two-Step (18) F Labeling Strategy for (18) F-PARP1 Inhibitors. ChemMedChem. 2011; 6(3):424–427. [PubMed: 21360818]
26. Reiner T, Earley S, Turetsky A, Weissleder R. Bioorthogonal small-molecule ligands for PARP1 imaging in living cells. ChemBioChem. 2010; 11(17):2374–2377. [PubMed: 20967817]
27. Reiner T, Keliher EJ, Earley S, Marinelli B, Weissleder R. Synthesis and In Vivo Imaging of a (18) F-Labeled PARP1 Inhibitor Using a Chemically Orthogonal Scavenger-Assisted High-Performance Method. Angew Chem Int Ed Engl. 2011; 50(8):1922–1925. [PubMed: 21328671]
28. Devaraj NK, Hilderbrand S, Upadhyay R, Mazitschek R, Weissleder R. Bioorthogonal Turn-On Probes for Imaging Small Molecules inside Living Cells. Angew Chem Int Ed Engl. 2010; 49(16): 2869–2872. [PubMed: 20306505]
29. Weissleder R, Kelly K, Sun EY, Shtatland T, Josephson L. Cell-specific targeting of nanoparticles by multivalent attachment of small molecules. Nat Biotechnol. 2005; 23(11):1418–1423. [PubMed: 16244656]
30. Leimgruber A, Berger C, Cortez-Retamozo V, Etzrodt M, Newton AP, Waterman P, Figueiredo JL, Kohler RH, Elpek N, Mempel TR, Swirski FK, Nahrendorf M, Weissleder R, Pittet MJ. Behavior of endogenous tumor-associated macrophages assessed in vivo using a functionalized nanoparticle. Neoplasia. 2009; 11(5):459–68. 2 p following 468. [PubMed: 19412430]
31. Kelly KA, Shaw SY, Nahrendorf M, Kristoff K, Aikawa E, Schreiber SL, Clemons PA, Weissleder R. Unbiased discovery of in vivo imaging probes through in vitro profiling of nanoparticle libraries. Integr Biol (Camb). 2009; 1(4):311–317. [PubMed: 20023731]
32. Mammem M, Choi SK, Whitesides GM. Polyvalent interactions in biological systems: implications for design and use of multivalent ligands and inhibitors. Angew Chem Int Ed. 1998; 21:2754–2794.
33. Tassa C, Duffner JL, Lewis TA, Weissleder R, Schreiber SL, Koehler AN, Shaw SY. Binding affinity and kinetic analysis of targeted small molecule-modified nanoparticles. Bioconjug Chem. 2010; 21(1):14–19. [PubMed: 20028085]
34. Thurber GM, Schmidt MM, Wittrup KD. Factors determining antibody distribution in tumors. Trends Pharmacol. Sci. 2008; 29(2):57–61. [PubMed: 18179828]
35. Sosnovik DE, Nahrendorf M, Weissleder R. Magnetic nanoparticles for MR imaging: agents, techniques and cardiovascular applications. Basic Res Cardiol. 2008; 103(2):122–130. [PubMed: 18324368]
36. Tsourkas, A.; Josephson, L. Magnetic nanoparticles. In: Weissleder, R.; Ross, BD.; Rehemtulla, A.; Gambhir, SS., editors. Molecular Imaging: Principles and Practice. People's Medical Publishing House; USA: 2010. p. 523-541.
37. Perez JM, Josephson L, O'Loughlin T, Hogemann D, Weissleder R. Magnetic relaxation switches capable of sensing molecular interactions. Nat Biotechnol. 2002; 20(8):816–820. [PubMed: 12134166]
38. Lee H, Sun E, Ham D, Weissleder R. Chip-NMR biosensor for detection and molecular analysis of cells. Nat Med. 2008; 14(8):869–874. [PubMed: 18607350]
39. Lee H, Yoon TJ, Weissleder R. Ultrasensitive detection of bacteria using core-shell nanoparticles and an NMR-filter system. Angew Chem Int Ed Engl. 2009; 48(31):5657–5660. [PubMed: 19554581]
40. Perez JM, Josephson L, Weissleder R. Use of magnetic nanoparticles as nanosensors to probe for molecular interactions. ChemBioChem. 2004; 5(3):261–264. [PubMed: 14997516]

NIH-PA Author Manuscript

NIH-PA Author Manuscript

NIH-PA Author Manuscript

41. Grimm J, Perez JM, Josephson L, Weissleder R. Novel nanosensors for rapid analysis of telomerase activity. Cancer Res. 2004; 64(2):639–643. [PubMed: 14744779]
42. Kaittanis C, Naser SA, Perez JM. One-step, nanoparticle-mediated bacterial detection with magnetic relaxation. Nano Lett. 2007; 7(2):380–383. [PubMed: 17298004]
43. Perez JM, Grimm J, Josephson L, Weissleder R. Integrated nanosensors to determine levels and functional activity of human telomerase. Neoplasia. 2008; 10(10):1066–1072. [PubMed: 18813356]
44. Kaittanis C, Nath S, Perez JM. Rapid nanoparticle-mediated monitoring of bacterial metabolic activity and assessment of antimicrobial susceptibility in blood with magnetic relaxation. PLoS One. 2008; 3(9):e3253. [PubMed: 18810269]
45. Haun JB, Yoon TJ, Lee H, Weissleder R. Magnetic nanoparticle biosensors. Wiley Interdiscip Rev Nanomed Nanobiotechnol. 2010; 2(3):291–304. [PubMed: 20336708]
46. Kaittanis C, Santra S, Perez JM. Role of nanoparticle valency in the nondestructive magnetic-relaxation-mediated detection and magnetic isolation of cells in complex media. J. Am. Chem. Soc. 2009; 131(35):12780–12791. [PubMed: 19681607]
47. Kaittanis C, Banerjee T, Santra S, Santiesteban OJ, Teter K, Perez JM. Identification of molecular-mimicry-based ligands for cholera diagnostics using magnetic relaxation. Bioconjug Chem. 2011; 22(2):307–314. [PubMed: 21226491]
48. Haun JB, Castro CM, Wang R, Peterson VM, Marinelli BS, Lee H, Weissleder R. Micro-NMR for Rapid Molecular Analysis of Human Tumor Samples. Sci Transl Med. 2011; 3(71):71ra16.
49. Denis MC, Mahmood U, Benoist C, Mathis D, Weissleder R. Imaging inflammation of the pancreatic islets in type 1 diabetes. Proc. Natl. Acad. Sci. U. S. A. 2004; 101(34):12634–12639. [PubMed: 15304647]
50. Guimaraes AR, Rakhlin E, Weissleder R, Thayer SP. Magnetic resonance imaging monitors physiological changes with antihedgehog therapy in pancreatic adenocarcinoma xenograft model. Pancreas. 2008; 37(4):440–444. [PubMed: 18953259]
51. Guimaraes AR, Ross R, Figuereido JL, Waterman P, Weissleder R. MRI with Magnetic Nanoparticles Monitors Downstream Anti-Angiogenic Effects of mTOR Inhibition. Mol Imaging Biol. 2010
52. Hogemann D, Ntziachristos V, Josephson L, Weissleder R. High throughput magnetic resonance imaging for evaluating targeted nanoparticle probes. Bioconjug Chem. 2002; 13(1):116–121. [PubMed: 11792186]
53. Sosnovik DE, Weissleder R. Emerging concepts in molecular MRI. Curr. Opin. Biotechnol. 2007; 18(1):4–10. [PubMed: 17126545]
54. Jaffer FA, Nahrendorf M, Sosnovik D, Kelly KA, Aikawa E, Weissleder R. Cellular imaging of inflammation in atherosclerosis using magnetofluorescent nanomaterials. Mol Imaging. 2006; 5(2):85–92. [PubMed: 16954022]
55. Kelly KA, Bardeesy N, Anbazhagan R, Gurumurthy S, Berger J, Alencar H, Depinho RA, Mahmood U, Weissleder R. Targeted nanoparticles for imaging incipient pancreatic ductal adenocarcinoma. PLoS Med. 2008; 5(4):e85. [PubMed: 18416599]
56. Korosoglou G, Tang L, Kedziorek D, Cosby K, Gilson WD, Vonken EJ, Schar M, Sosnovik D, Kraitchman DL, Weiss RG, Weissleder R, Stuber M. Positive contrast MR-lymphography using inversion recovery with ON-resonant water suppression (IRON). J Magn Reson Imaging. 2008; 27(5):1175–1180. [PubMed: 18425827]
57. Korosoglou G, Weiss RG, Kedziorek DA, Walczak P, Gilson WD, Schar M, Sosnovik DE, Kraitchman DL, Boston RC, Bulte JW, Weissleder R, Stuber M. Noninvasive detection of macrophage-rich atherosclerotic plaque in hyperlipidemic rabbits using “positive contrast” magnetic resonance imaging. J Am Coll Cardiol. 2008; 52(6):483–491. [PubMed: 18672170]
58. Montet X, Weissleder R, Josephson L. Imaging pancreatic cancer with a peptide-nanoparticle conjugate targeted to normal pancreas. Bioconjug Chem. 2006; 17(4):905–911. [PubMed: 16848396]
59. Morishige K, Kacher DF, Libby P, Josephson L, Ganz P, Weissleder R, Aikawa M. High-resolution magnetic resonance imaging enhanced with superparamagnetic nanoparticles measures

NIH-PA Author Manuscript

NIH-PA Author Manuscript

NIH-PA Author Manuscript

macrophage burden in atherosclerosis. Circulation. 2010; 122(17):1707–1715. [PubMed: 20937980]

60. Nahrendorf M, Jaffer FA, Kelly KA, Sosnovik DE, Aikawa E, Libby P, Weissleder R. Noninvasive vascular cell adhesion molecule-1 imaging identifies inflammatory activation of cells in atherosclerosis. Circulation. 2006; 114(14):1504–1511. [PubMed: 17000904]
61. Schellenberger EA, Sosnovik D, Weissleder R, Josephson L. Magneto/optical annexin V, a multimodal protein. Bioconjug Chem. 2004; 15(5):1062–1067. [PubMed: 15366960]
62. Sosnovik DE, Garanger E, Aikawa E, Nahrendorf M, Figuiredo JL, Dai G, Reynolds F, Rosenzweig A, Weissleder R, Josephson L. Molecular MRI of cardiomyocyte apoptosis with simultaneous delayed-enhancement MRI distinguishes apoptotic and necrotic myocytes in vivo: potential for midmyocardial salvage in acute ischemia. Circ Cardiovasc Imaging. 2009; 2(6):460–467. [PubMed: 19920044]
63. Sosnovik DE, Nahrendorf M, Panizzi P, Matsui T, Aikawa E, Dai G, Li L, Reynolds F, Dorn G. W. n. Weissleder R, Josephson L, Rosenzweig A. Molecular MRI detects low levels of cardiomyocyte apoptosis in a transgenic model of chronic heart failure. Circ Cardiovasc Imaging. 2009; 2(6):468–475. [PubMed: 19920045]
64. Sosnovik DE, Schellenberger EA, Nahrendorf M, Novikov MS, Matsui T, Dai G, Reynolds F, Grazette L, Rosenzweig A, Weissleder R, Josephson L. Magnetic resonance imaging of cardiomyocyte apoptosis with a novel magneto-optical nanoparticle. Magn Reson Med. 2005; 54(3):718–724. [PubMed: 16086367]
65. Turvey SE, Swart E, Denis MC, Mahmood U, Benoist C, Weissleder R, Mathis D. Noninvasive imaging of pancreatic inflammation and its reversal in type 1 diabetes. J. Clin. Invest. 2005; 115(9):2454–2461. [PubMed: 16110329]
66. Nahrendorf M, Keliher E, Marinelli B, Waterman P, Feruglio PF, Fexon L, Pivovarov M, Swirski FK, Pittet MJ, Vinegoni C, Weissleder R. Hybrid PET-optical imaging using targeted probes. Proc. Natl. Acad. Sci. U. S. A. 2010; 107(17):7910–7915. [PubMed: 20385821]
67. Nahrendorf M, Keliher E, Marinelli B, Leuschner F, Robins CS, Gerszten RE, Pittet MJ, Swirski FK, Weissleder R. Detection of Macrophages in Aortic Aneurysms by Nanoparticle Positron Emission Tomography-Computed Tomography. Arterioscler Thromb Vasc Biol. 2011
68. Santra S, Kaittanis C, Grimm J, Perez JM. Drug/dye-loaded, multifunctional iron oxide nanoparticles for combined targeted cancer therapy and dual optical/magnetic resonance imaging. Small. 2009; 5(16):1862–1868. [PubMed: 19384879]
69. Kievit FM, Zhang M. Surface Engineering of Iron Oxide Nanoparticles for Targeted Cancer Therapy. Acc. Chem. Res. 2011
70. Ethirajan M, Chen Y, Joshi P, Pandey RK. The role of porphyrin chemistry in tumor imaging and photodynamic therapy. Chem. Soc. Rev. 2011; 40(1):340–362. [PubMed: 20694259]
71. Spikes JD. Chlorins as photosensitizers in biology and medicine. J Photochem Photobiol B. 1990; 6(3):259–274. [PubMed: 2120404]
72. McCarthy JR, Jaffer FA, Weissleder R. A macrophage-targeted theranostic nanoparticle for biomedical applications. Small. 2006; 2(8-9):983–987. [PubMed: 17193154]
73. McCarthy JR, Korngold E, Weissleder R, Jaffer FA. A light-activated theranostic nanoagent for targeted macrophage ablation in inflammatory atherosclerosis. Small. 2010; 6(18):2041–2049. [PubMed: 20721949]

NIH-PA Author Manuscript

NIH-PA Author Manuscript

NIH-PA Author Manuscript

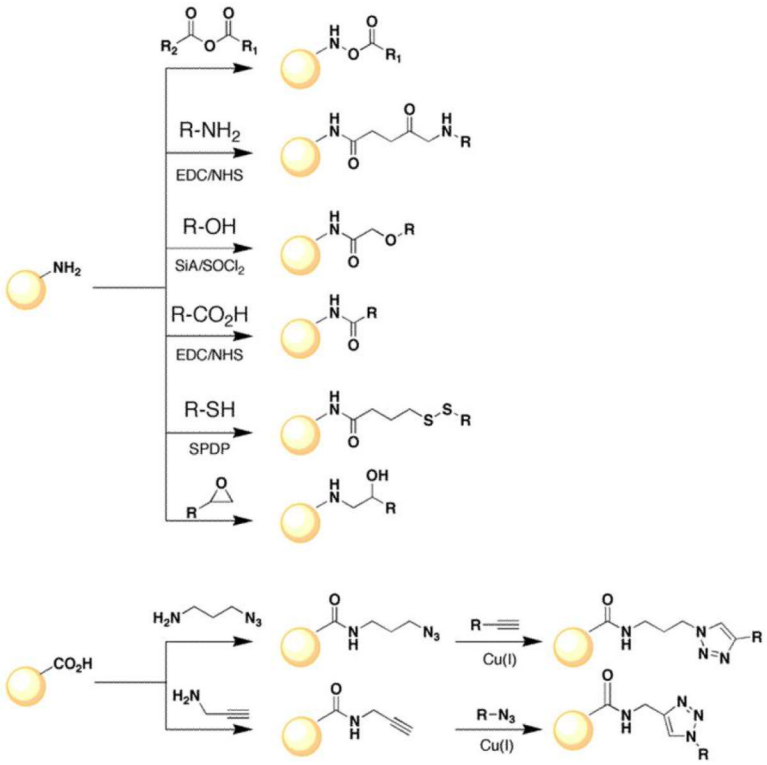

Figure 1.
Conjugation chemistries to attach small molecules to CLIO. From ref (21).

NIH-PA Author Manuscript

NIH-PA Author Manuscript

NIH-PA Author Manuscript

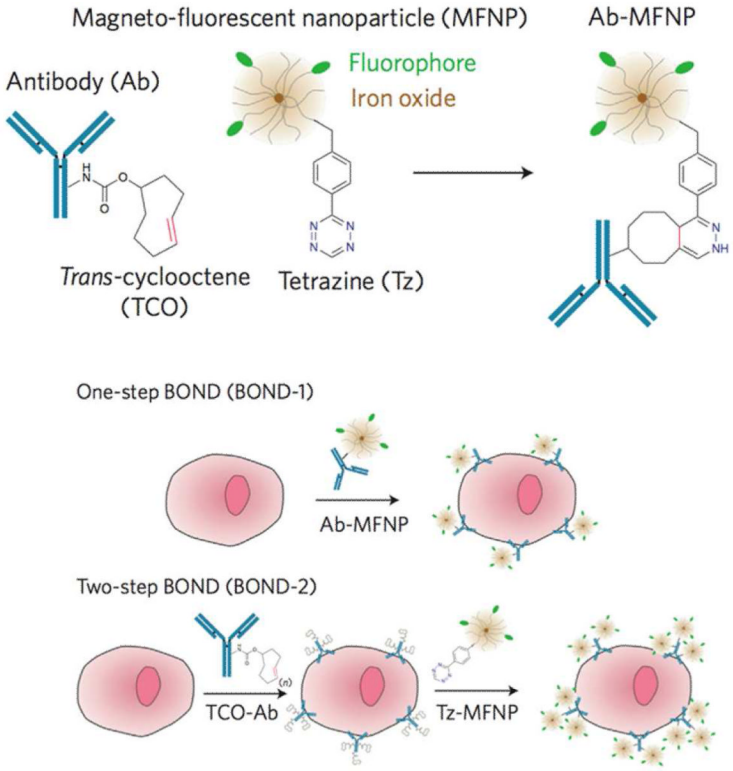

Figure 2.
Bioorthogonal [4 + 2] cycloaddition reaction between 1,2,4,5-tetrazene (Tz) and *trans*-cyclooctene (TCO) for labeling of nanoparticles (top) or cell surfaces (bottom). From ref (27).

NIH-PA Author Manuscript

NIH-PA Author Manuscript

NIH-PA Author Manuscript

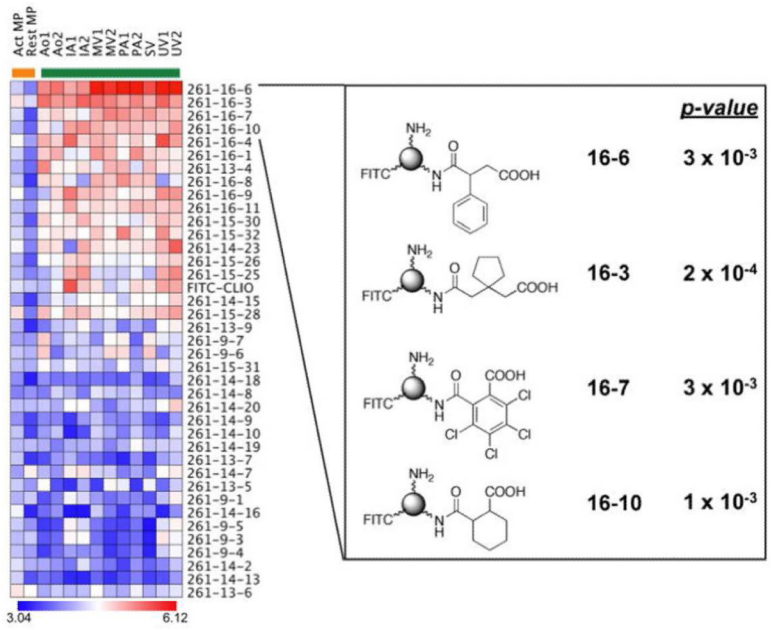

Figure 3.
Screening for small-molecule-modified nanoparticles with enhanced binding to 11 independent endothelial isolates (relative to macrophage binding). From ref (23).

NIH-PA Author Manuscript

NIH-PA Author Manuscript

NIH-PA Author Manuscript

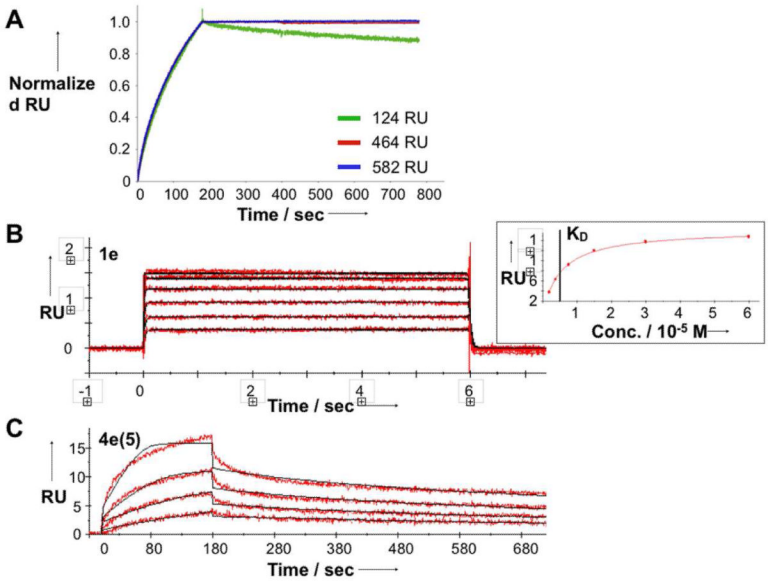

Figure 4.

Surface plasmon resonance to quantitate kinetics and affinity of nanoparticle binding. A. At high target densities (e.g. 464 and 582 RU, or response units), there is negligible dissociation of multivalent nanoparticles. B. and C. SPR reveals distinct kinetics for interaction of a protein target with its free small molecule ligand (B) vs a multivalent nanoparticle conjugated to the ligand (C). From ref (25).

NIH-PA Author Manuscript
NIH-PA Author Manuscript
NIH-PA Author Manuscript

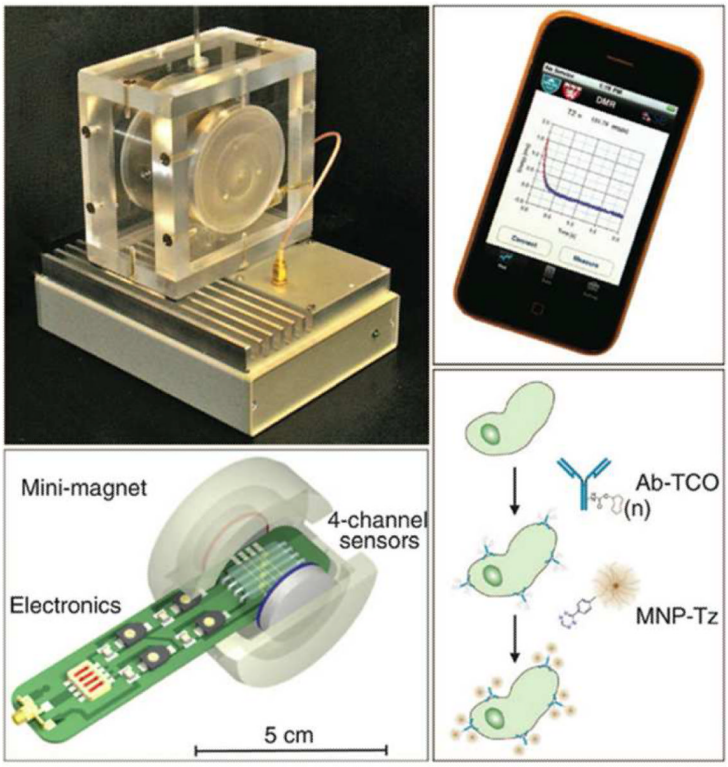

Figure 5.
μNMR diagnostic magnetic resonance (DMR) device. Point-of-care μNMR device (top left) containing circuitry for NMR measurements (bottom left) is controlled by a smart phone application. Detection of cellular receptors via magnetic nanoparticles and BOND bioorthogonal conjugation is shown at bottom right. From ref (35).

NIH-PA Author Manuscript

NIH-PA Author Manuscript

NIH-PA Author Manuscript

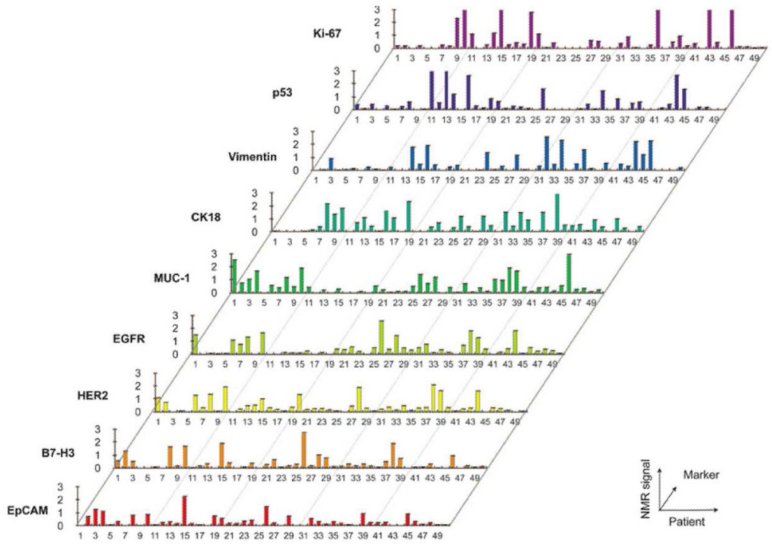

Figure 6.
Profiling of cancer marker expression from 50 patient FNAs using DMR. From ref (35).

NIH-PA Author Manuscript

NIH-PA Author Manuscript

NIH-PA Author Manuscript

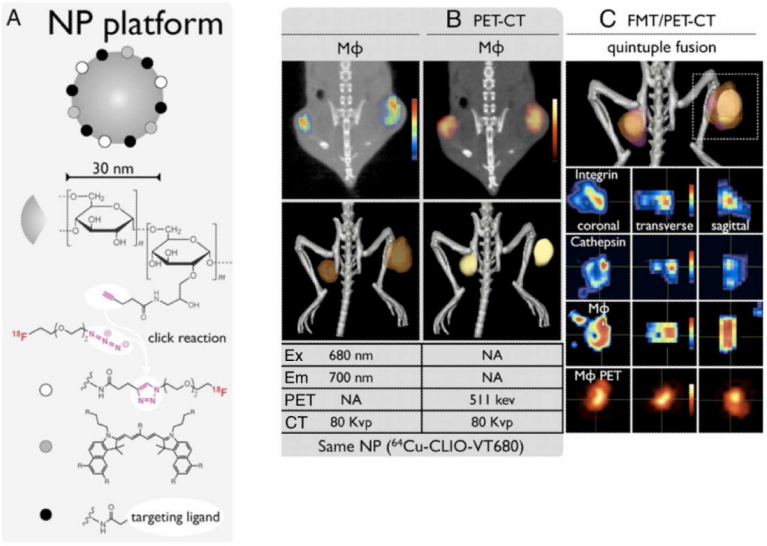

Figure 7.

Multimodal PET imaging using nanoparticles. A. Versatile conjugation capabilities of CLIO, e.g. to ^{18}F using click chemistry, but also to peptides or other targeting ligands. B and C. In vivo multichannel PET-CT (B) and FMT/PET-CT (C) of tumor-bearing mice, co-injected with fluorescent peptide against integrins, a fluorescent cathepsin sensor, and ^{64}Cu-CLIO-VT680 (labeling macrophages). From ref (55).

NIH-PA Author Manuscript

NIH-PA Author Manuscript

NIH-PA Author Manuscript

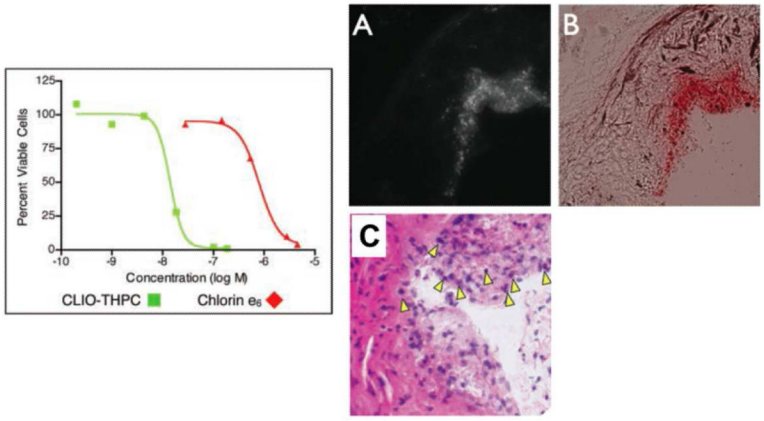

Figure 8.

Nanoparticle-based theranostic agent for photodynamic therapy. (Left) Theranostic nanoparticle enhances phototoxicity vs. chlorin e_6. (Right) CLIO-THPC localizes to atheroma of apoE$^{-/-}$ mice, as evidenced by fluorescent microscopy of nanoparticle (A), merged fluorescent-bright field microscopy (B), and areas of apoptotic and necrotic cells (C). From ref (60).